Transverse shear measurement for corrugated board and its significance

ROMAN E. POPIL[1], DOUGLAS W. COFFIN[2] AND CHARLES C. HABEGER[3]

SUMMARY

When a corrugated box is placed under vertical load the panel walls will deform out of plane and the propensity of the linerboard facings to move with respect to one another in this and similar situations is described by the transverse shear rigidity of the corrugated board. This has been a neglected property in the corrugated industry and is not measured routinely in manufacturing environments. However, loss of stacking strength in corrugated containers can potentially be attributed to the loss of transverse shear rigidity, and this loss can easily result during converting. Diminished transverse shear resistance cannot be measured through usual quality measurements such as board caliper or flexural rigidity). For example, a typical 10 % loss of caliper from board crushing which arises from the press feed roll results in a 20% reduction in flexural rigidity and a corresponding 65% loss in transverse shear rigidity. A loss in shear rigidity of this magnitude will affect the stacking strength more so than predicted from only the combined loss of flexural rigidity or caliper and ECT. A method of measuring the MD and CD transverse shear as well as the twisting stiffness using a mechanical method of a torsional pendulum is described and demonstrated on a selected variety of corrugated boards. The sensitivity of the measurement to board crushing is shown by corresponding flat crush hardness values.

INTRODUCTION

The main structural advantage of corrugated board is the high ratio of bending stiffness to weight. This is accomplished by the fluted medium that provides spacing between liners to increase the bending stiffness of the combined board in proportion to the square of the spacing. Cross Direction, CD, compressive strength is the primary material property that receives focus from the industry by routine measurement of Short Span Compression strength (SCT), Edge Crush (ECT), or Box Compression (BCT). A third property, transverse shear stiffness, has received limited attention from the industry in North America and is usually not considered in the design of the box. However, when a corrugated box is vertically loaded, panel bending and shearing both lead to post-buckling deformation that concentrate load in the box corners. Box corners are usually where a compressive failure in the form of a crease initiates from the concentration of combined compressive and shear stresses and then propagates across the panels causing collapse of the box.

The fluting medium influences CD properties differently than MD properties, which can be appreciated through examination of Figure 1. For both the medium and liners, the MD compressive strength is higher than that in the CD due to fiber orientation. However, for combined board strength, the fluted medium contributes its CD strength weighted by the medium to liner length ratio or "take-up" factor which in the case for C flute is about 1.42, and combined board strength is highest in the CD. On the other hand for, bending stiffness, the fluting direction plays a minor role in MD and CD differences, and the bending stiffness of corrugated board is actually always higher in the MD than in the CD because the liners are stiffer in the MD. The role of the fluting is largely to provide a separation between the liners. In contrast, fluting direction will have a major impact on transverse shear stiffness and MD and CD differences will be large.

If a corrugated board, as shown in Figure 1, is subjected to shearing action such that the top liner is displaced in-plane relative to the bottom liner with a shearing motion, the MD resistance would be much lower than the CD resistance. Transverse shear stiffness is the resistance of the board to shearing motion in the MD-ZD plane or the CD-ZD plane. This quantity expressed as a rigidity (stiffness times the board caliper) is ascribed the symbol R_{55} for the MD-ZD plane and R_{44} for the CD-ZD plane.

The other important shear resistance is that which restricts shear in the MD-CD plane. For corrugated board the in-plane shear stiffness of the liners impacts the twisting bending stiffness, which is ascribed the symbol D_{66}.

If the corrugated board is regarded as a sandwich plate, these three shear stiffnesses are properties that characterize the ability of the board to restrict shear deformation. Shear deformation plays a role in the bending response of the box. A low MD-ZD or simply MD transverse shear stiffness would lower the bulging resistance of stacked boxes and negatively impact box lifetime. On the other hand, the low shear resistance improves the ability of the board to be scored, creased, and folded. It is believed that transverse shear stiffness plays a bigger role in box lifetime under conditions of cyclic moisture than has been previously attributed. Transverse shear of corrugated board is more sensitive to flat crushing of the board and may help explain in part why crushing the board lowers BCT more so than predictions based solely on ECT and bending stiffness alone (*1*). Indeed, theoretical calculations based on elasticity theory, the results of which will be pre-

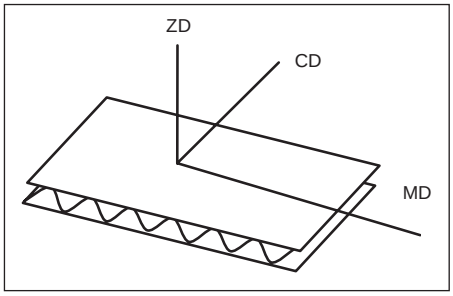

Fig. 1 Directional assignments of corrugated board. x,y,z = 11, 22, 33 = MD,CD, and ZD respectively.

[1]Senior Research Scientist and corresponding author (Roman.Popil@ipst.gatech.edu)
Georgia Institute of Technology
Institute of Paper Science and Technology
Atlanta, Georgia.
[2]Associate Professor
Miami University
Pulp and Paper Engineering
Oxford, Ohio.
[3]Charles C. Habeger
Scientific Advisor
Weyerhaeuser Company,
Federal Way, Washington.

sented here, indicate that loss of transverse shear stiffness from crushing will have a significant effect on the buckling resistance of the panels of a corrugated box. Accounting for the shear stiffness gives the industry another property with which to characterize the board and better predict performance.

Combined board out-of-plane shear rigidities have been measured by shear block test and by three point bending methods (*2*). These measurements were used to explain the difference between the measured and predicted buckling load of a 15 x 15 mm corrugated board panel since the numerical and analytical models for the panel buckling load did not include transverse shear of the panel. Other methods have been developed (*3,4*) based on the measurement of torsional stiffness. The moment applied to twist a 25 x 100 mm specimen is measured to a specified angle and related to the transverse shear rigidity through an analysis and numerical modeling. Similar to the present treatment, a commercial instrument is available that measures the angular frequency of the twisting oscillation and calculates a torsional stiffness (*5*). Another recently developed instrument is based on a nondestructive vibrator excitation of the resonant frequency of an MD-ZD induced shear mode of deformation (*6*). This paper describes a torsional pendulum developed to measure the torsional stiffness of board samples. These properties are determined by recording the transient dynamic response of the torsion pendulum after an initial displacement of the test specimen. A computer analysis that accounts for the inherent damping of the system obtained in a calibration step obtains the twisting frequency and the damping characteristics of the combined board. An experimental torsional stiffness of the board is then calculated. Three shear properties, the transverse shear rigidities R_{55}, R_{44} and the twisting bending stiffness D_{66}, are obtained from the accumulated torsional stiffness data for samples of several widths cut in the MD and CD utilizing a previous analytic result (*7*). An approximate method using fewer samples but incorporating a separate measure of four-point bending stiffness is also presented.

Preliminaries

For a beam of length L subjected to torsion, as shown in Figure 2, the torsional stiffness is related to the torque, T, and angle of twist, θ, as follows:

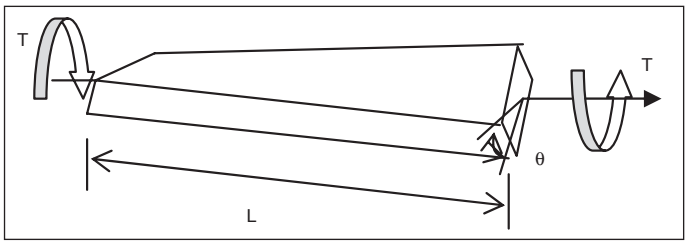

Fig. 2 Torsion of a beam of length L and angular displacement θ.

$$k = \frac{T}{\theta} \qquad [1]$$

The corrugated board is represented as an orthotropic plate with a constitutive equation given as

$$\begin{Bmatrix} M_{xx} \\ M_{yy} \\ M_{xy} \\ Q_{yz} \\ Q_{xz} \end{Bmatrix} = \begin{bmatrix} D_{11} & D_{12} & 0 & 0 & 0 \\ D_{12} & D_{22} & 0 & 0 & 0 \\ 0 & 0 & D_{66} & 0 & 0 \\ 0 & 0 & 0 & R_{44} & 0 \\ 0 & 0 & 0 & 0 & R_{55} \end{bmatrix} \begin{Bmatrix} \kappa_{xx} \\ \kappa_{yy} \\ \kappa_{xy} \\ \gamma_{yz} \\ \gamma_{xz} \end{Bmatrix} \qquad [2]$$

where the M_{ij}'s and Q_{ij}'s are distributed moments and shear forces respectively, κ_{ij} are the curvatures, γ_{ij} are the transverse shear strains, D_{ij}'s are the bending stiffnesses, and R_{ii} are the shear rigidities. Equation [2] is the starting basis for calculating the potential effects of transverse shear on box properties as will be discussed later in this document. The properties of interest for the immediate current discussion are the three shear terms, D_{66}, R_{44}, and R_{55}. For a sandwich structure similar to corrugated board the twisting bending stiffness is approximately

$$D_{66} \cong \frac{1}{2} G_{xy} t h^2 \qquad [3]$$

where G_{xy} is the in-plane shear stiffness of the liners, t is the thickness of the liners, and h is the thickness of the sheet. Equation [3] retains only the dominant term in the expression for a sandwich structure where the direct contribution of the sandwich core properties are assumed to be negligible.

There have been several analytical models in the literature for the prediction of torsional stiffness of beams and plates, the one proposed by Reissner (*8*) is adapted for our purposes here. In this case, the plate solution for the torsional problem can be expressed as

$$\frac{T}{\theta}_{\text{Reissner}} = \frac{4 D_{66} b}{L\left(1 + 12 \frac{D_{66}}{R_{55} b^2}\right)} = k_{MD} \qquad [4]$$

where the length of the plate L is assumed to be large compared to the width b and thickness Similarly, when specimens are cut with their flutes parallel to their length L the twisting stiffness k_{CD} is measured and the torsional stiffness can be written as

$$\frac{T}{\theta}_{\text{Reissner}} = \frac{4 D_{66} b}{L\left(1 + 12 \frac{D_{66}}{R_{44} b^2}\right)} = k_{CD} \qquad [5]$$

Equations [4,5] derived using plate mechanics were found to match well with the finite-element results reported by McKinlay (*4*) which modeled the medium and linerboards separately.

Thus using Equations [4,5] with the measurement of the torsional stiffness one can extract estimates of the relevant shear rigidities and bending stiffness.

In our procedure, L is 24 cm and b is 7.6 cm or less.

The torsion pendulum method

The torsion pendulum consists of a gusseted bar frame structure which supports the sample clamps. The bottom clamp is affixed to a flange on which rests a dumbbell of 20 kg weights supported by a platform bearing to reduce twisting friction. A permanent magnet affixed to the rotating flange with a Hall effect sensor on the supporting platform translate the oscillatory motion of the assembly measured as a time varying deflection angle to an electrical signal which is digitized by a PC fitted with a Labview digitizer card. The differential equation for angular deflection $\theta(t)$, which governs pendulum rotation of the twisting sample is

$$I \frac{d^2\theta}{dt^2} + r \frac{d\theta}{dt} + k_p \theta = 0 \qquad [6]$$

so that the complex resonant frequency ($\omega_r + i\omega_i$) of the oscillating linear pendulum depends on the mass radial moment of inertia of the pendulum I, the frictional drag coefficient, r, of the pendulum and the complex angular spring constant of the sample, k_p.

Fig. 3 Photograph of the IPST torsion pendulum consisting of a freely rotating dumbbell fitted with a Hall effect sensor and clamps holding a twisting board test specimen.

Ideally, the deflection angle versus time plots will be perfect exponentially damped sinusoidal curves:

$$\theta(t) = \cos(\omega_r t + \delta)e^{-\omega_i t} \qquad [7]$$

where ω_r represents the resonant frequency of pendulum, ω_i is the attenuation coefficient, and δ is a phase shift depending on the pendulum release time. The pendulum was designed to allow direct determination of k through the observation of the damped oscillations once the pendulum loaded with a test sample is set in motion.

A pendulum calibration procedure consists of using a steel sheet metal strip in place as the test specimen and recording the angular deflections with known applied torques via a simple pulley and weight system to determine the metal plate spring constant. The pendulum moment of inertia I and damping factor r are then calculated though fitting the damped oscillation curve obtained with the calibrating metal plate set into twisting oscillation. The resonant frequency of the oscillations is determined through calculation using a Fourier technique (*7*) previously implemented for torsion pendulum analysis. This calibration procedure calculates the I and r of the system and produces k's in units of N-m/radian.

Samples of corrugated board are cut in widths varying from 3 inches to 1.5 inches and placed in the jaws of the torsion pendulum shown in Figure 3. Corrugated board test specimens have their terminating ends filled with tightly fitting steel dowels and firmly secured in the top and bottom clamps. The pendulum is given a horizontal displacement of 20 degrees and the Hall probe records the twisting oscillations of the sample once is released. To obtain k_{MD}, samples are cut so that the flutings are perpendicular to the length of the test specimen. Figure 4 shows the typical waveform from the damped twisting oscillations of a sample and the resulting computer fitting and output.

Determination of Shear Properties from Torsional Stiffness data.

The torsion pendulum provides values of the torsional stiffness k_{MD} or k_{CD} as a function of the sample width b. Utilizing values of k for a specimen type as a function of sample width, Equations [4] and [5] are fit to the data (b,k) to obtain the three shear properties D_{66}, R_{55}, and R_{44} that minimize the sum of the squared error.

Figure 5 shows results from several commercial boards and one in-house produced board made at the IPST pilot corrugator. The typical coefficient of variation of measured k's is about 6%.

Inspection of Figure 5 shows immediately that the torsional stiffness in the MD is much less than the CD for all samples except the E flute where the combination of spacing and height of the flutings is such that it acts more like a continuum rather than a sandwich structure. The basis weights in lb/1000 ft^2 of the linerboards and fluted medium with type designated by letter are provided in the legend, "I" and "W" are commercial boards and "IEC" board was produced at IPST on a pilot corrugator. The best fit for the shear rigidities and twisting bending stiffness are given in the left side of Table 1.

From Equation [3], it can be appreciated why D_{66} is low for the E flute sample since the caliper of E flute is much lower than that of C flute by about a factor of 2.6. Boards that have 56 lb/msf liners can be expected to have higher D_{66} values than those of lower basis weight since the in-plane moduli E_i of liners generally scales with basis weight. This latter statement can be appreciated given the bending and twisting stiffness approximations for the case of a sandwich beam structure consisting of plates of thickness t separated by a distance h

$$D_{11} \cong \frac{E_x t h^2}{2(1-\nu_m^2)}, \quad D_{22} \cong \frac{E_y t h^2}{2(1-\nu_m^2)} \qquad [8]$$

where E_x, E_y are the in-plane moduli of the liners and, ν_m is the geometric mean in-plane Poisson ratio, D_{11}, D_{22} in-plane bending stiffness of the combined board. D_{66} was given in Equation [3]. Equations

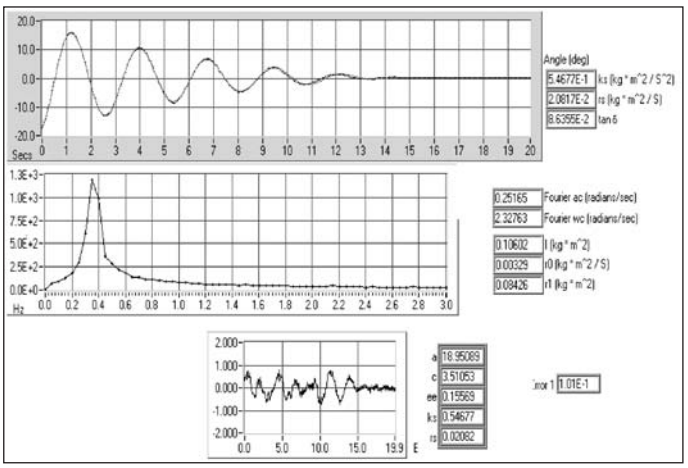

Fig. 4 Typical damped twisting oscillation waveform (top graph) and damped oscillator model fit results (resonant frequency middle graph) for a combined board sample torsion pendulum test.

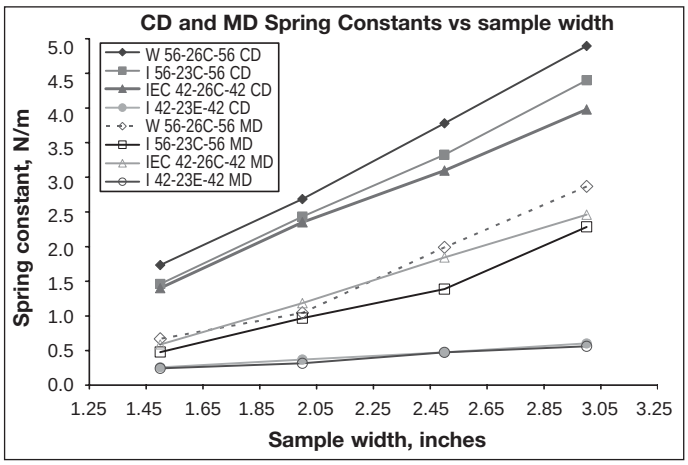

Fig. 5 Results from the torsional pendulum, torsional spring constants as a function of sample width.

[3] and [8] retain only the dominant term of the actual full expressions for a sandwich beam. Moreover, Baum (*9*) showed an approximate relationship between the liner in-plane shear modulus and the in-plane moduli to be

$$G_{xy} \cong 0.387\sqrt{E_x E_y} \qquad [9]$$

From Equation [9] it can be inferred that ν_m =0.293.

By combining Equation [9] with [8] we find that we can check the values for D_{66} knowing the geometric mean bending stiffness $\sqrt{(D_{11}\ D_{22})}$ ("GM") from a 4-point bending measurement of the combined board thus:

$$D_{66} \cong 0.354\sqrt{D_{11}D_{22}} \qquad [10]$$

Indeed, if we take the example of the IEC 42-26C-42 board, the measured geometric mean bending stiffness is 10.6 N-m and Equation [10] predicts D_{66} = 3.75 N/m which is comparable to the value of D_{66} = 3.5 N/m obtained with the torsion pendulum.

Therefore an approximation for R_{55} using strips of a single width can be obtained from solving Equation [4] as

$$R_{55} = \frac{12D_{66}}{\left(4\frac{D_{66}b}{k_{MD}L}-1\right)b^2} \qquad [11]$$

and utilizing Equation [10] for D_{66}.

Similarly, by substituting k_{CD} for k_{MD} in Equation [11] we can determine R_{44}.

A comparison of Equation [4] and [10] using MD and CD strips of 5 different widths for a total of 50 measurements is provided in Table 1. MD transverse shear rigidity is measured using the IPST torsion pendulum using strips of 6.4 cm width cut along the MD of the board with *L* being 23 cm.

Therefore, a preferred convenient method of determining R_{55} at the loss of some accuracy is to measure the spring constant of corrugated board sample of width *d* and length *L* followed by a measure of its MD and CD bending stiffness by the 4 point method. Substituting bending stiffness values into Equation [10] for D_{66} along with torsional spring constant *k* allows calculation of R_{55} using Equation [11]. Note, if D_{66} is small relative to the R_{44} and R_{55}, there is low significance to the transverse shear stiffness values, but transverse shear deformation is also not important in these instances. When the values of R_{55} are all high, MD transverse shear stiffness is not important so the value of D_{66} dominates the torsional response. By example, in Table 1, the E-flute board (I42-23E) has such a low estimated value of D_{66} that a value of shear stiffness can not be computed from Equation [11].

Table 1
Results from fitting spring constant kMD, kCD data to analytic expression, Equations [4] and [5] and an approximate single width method Equation [11].

Sample ID	D_{66} N-m	R_{55} N/m	R_{44} N/m	GM N-m	D_{66}[1] N-m	R_{55}[2] N-m by [11]
W56-25C	4.53	9330	53100	13.4	4.74	8650
I56-23C	4.14	6480	42800	11.6	4.11	5380
IEC4226C	3.54	9760	54300	10.6	3.75	8950
I42-23E	0.49	10900	20000	1.2	0.42	
IEC4226C After nip crush	3.27	3410	23300			

GM= $\sqrt{D_{11}D_{22}}$, [1] from Equation [10], [2] from Equation [11]

Effect of crushing on corrugated board.

Table 1 provide shear parameters prior and after nip crushing for board IEC 42-26C-42. The value of the MD transverse shear rigidity, R_{55}, drops from 9760 to 3410. The CD transverse shear rigidity R_{44} is affected less by crushing, it correspondingly drops from 54300 to 23300 N-m. These changes are significant considering variability in repetitions of the measurements is about 6%. Equally important is that the value of D_{66} dropped by less than 10% since this quantity is largely influenced by the stiffness of the linerboards which are unaffected by crushing. Finding R_{55} using [11] results in a coefficient of variation of 12% typically. The samples in this crushing effect study were sent through a nip consisting of a chromed and rubber covered roll set to 70% of the nominal initial caliper. Immediately after passing through the nip, the caliper of the board was found to be reduced by 20% from its initial value. After 24 hour conditioning in a 50% RH environment, the permanent caliper reduction was measured to be 9 % which is also the margin of error of measurements in production. The remarkable recovery of combined board caliper from crush has been observed previously in the literature (*10-12*). Bending stiffness in this experiment was measured to be reduced by 21% consistent with the idea that bending stiffness is proportional to square of the liner separation [8] and that 4-point bending is unaffected by transverse shear. However, the loss in MD transverse shear can further affect a loss in the panel buckling load, and this is not accounted for in the usual predictive equation for *BCT*.

Recall that the McKee (*13*) equation for box compression strength, *BCT*, has the form:

$$BCT \propto ECT^{0.75}\left\{\sqrt{D_{11}D_{22}}\right\}^{0.25} W^{0.5} \qquad [12]$$

where the term $\sqrt{D_{11}D_{22}}$ is the geometric mean flexural rigidity of the board and *W* is the perimeter. The bending stiffness term arises from consideration that panel buckling affects strength. McKee did not consider transverse shear effects, and a more complete expression for the buckling load of a panel that does incorporate transverse shear (*14-17*) may be derived. A summary of this analysis is given in Appendix A. Ultimately, the analysis leads to the buckling load P of the loaded plate of width a and height b as:

$$P = \frac{\pi^2\sqrt{D_{11}D_{22}}}{a^2}m^2\left\{x^2 + 2\alpha + \frac{1}{x^2} - \frac{(x^2+\alpha)^2}{R+x^2+\beta}\right\} \qquad [13]$$

where

$$x = \sqrt[4]{\frac{D_{11}}{D_{22}}}\left(\frac{b}{a}\right)\left(\frac{m}{n}\right),\ \alpha = \frac{D_{12}+2D_{66}}{\sqrt{D_{11}D_{22}}},\ \beta = \frac{D_{66}}{\sqrt{D_{11}D_{22}}},$$

$$R = \frac{R_{55}b^2}{n^2\sqrt{D_{11}D_{22}}\pi^2},\ D_{12} = \nu_m\sqrt{D_{11}D_{22}}$$

The number of half waves in panel buckling, *m*, is taken to be one to find the lowest possible buckling load. The first three terms inside the curly braces of [13] are the buckling terms derived with no transverse shear as quoted by McKee in 1963 referred to as the "buckling coefficient" and further approximated by McKee to yield the more familiar form of the BCT Equation [12]. The Baum approximation (*9*) gives α=1 and β=0.354.

The ratio of the critical load with MD transverse shear P to the critical load with no transverse shear is written from Equation [13] as:

$$K_{plate} = \left\{ 1 - \frac{\left[x^2 + \alpha\right]^2}{\left(x^2 + 2\alpha + \frac{1}{x^2}\right)\left(x^2 + \beta + R\right)} \right\} \quad [14]$$

Consider now the effect that crushing has on the reduction of critical load. Table 2 provides values of pertinent numbers before and after crushing for a square box with a = 20 cm. Values for the bending stiffnesses and R_{55} were measured for the case of another C flute board sample set crushed to 70% of its original caliper.

The K values indicate that transverse shear has a significant effect on the critical buckling load even with no crushing however, crushing causes an additional 25% loss of buckling resistance due to loss of transverse shear rigidity. Thus the critical buckling load is lowered by 37% whereas without shear the buckling load decrease from crushing is only 16%. This example corresponds to crushing of a combined board such that it has lost 9% of its original caliper. Previous observations of 10% caliper permanent reduction from board crushing (*11*) show that this results in about a 10% loss in ECT value. The McKee BCT equation [12] predicts a loss of 11% in BCT for these circumstances. However, when the loss of shear in incorporated into [12] by using [13] the calculated BCT loss becomes 17%. Although this 17% loss of BCT is likely to be significant, only about a third of the loss is due directly to the loss of shear. Arguably, the effect of transverse shear deformation may be difficult to verify experimentally given the high variability of the BCT test (Tappi 804 Compression Test of Fiberboard Shipping Containers) and the known effects of crushing on ECT measurement (*18*). However, since the loss in BCT for these conditions is consistent with the loss in transverse shear stiffness of about 20%, transverse shear stiffness may prove to be a useful indicator of box quality in manufacturing operations which augurs well for the development of shear measurement instrumentation for quality control.

Table 2
Effect of crushing on shear and bending parameters

Sample	R_{55} N/m	$\sqrt{D_{11}D_{22}}$ N-m	K_{plate}	$\frac{P}{P_{no\ crush}}$	$\frac{BCT}{BCT_{no\ crush}}$
No crush	7675	12.2	0.671	1	1
Nip Crush	2787	10.3	0.505	0.63	0.82

b=20 cm, D_{11}/D_{22} = 2, $\frac{ECT_{crush}}{ECT_{no\ crush}}$ = 0.9

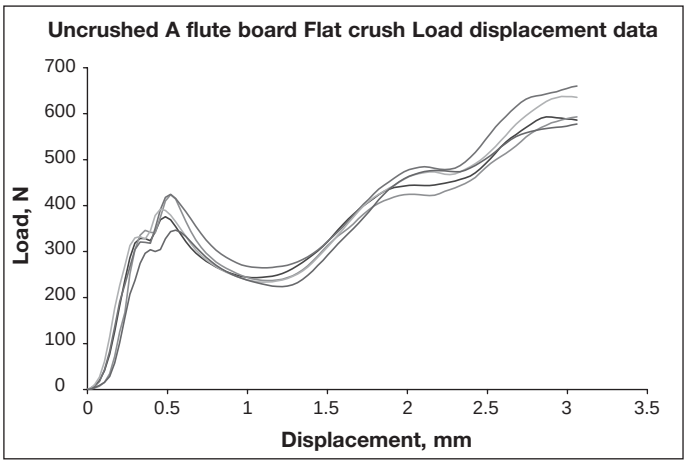

Fig. 6 Multiple flat crush load vs displacement curves, Newton vs mm displacement for uncrushed A flute board.

Correspondence of transverse shear loss with flat crush hardness

Combined board of A and C flute were crushed by running through a hard rubber nip set at 70% of the uncrushed nominal caliper. Flat crush load displacement data were obtained on a universal compression test frame and are shown in Figures 6 and 7 for the case of the A flute boards. The data for several repeat specimens are shown in each figure. Specimens were 2 x 2 inch squares as conventionally pre-

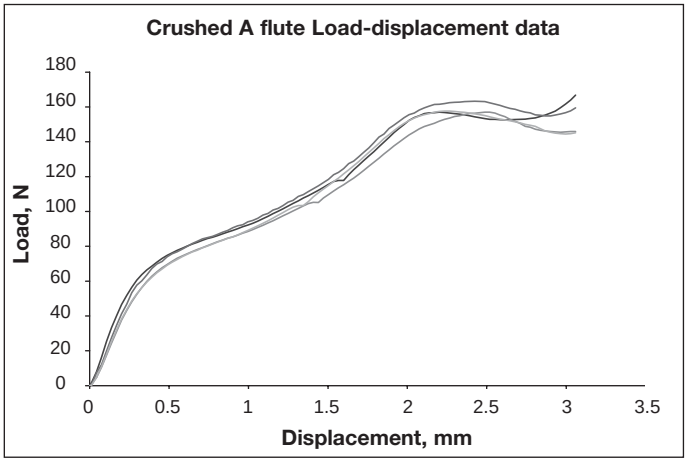

Fig. 7 Multiple load displacement curve for a series of crushed A flute boards showing a pronounced lowering of the first peak value or "hardness". Compare to Figure 6.

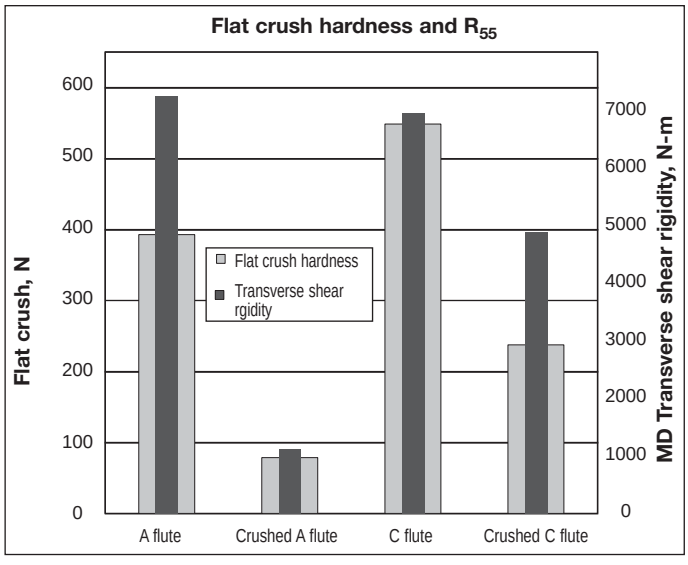

Fig. 8 Comparison of the flat crush hardness values and the transverse MD shear rigidity.

pared for ECT (Tappi 839) testing. The first peak in such load displacement curves has been dubbed by Crisp et al. (*19*) as the board "hardness" and has been shown to be sensitive to the damage sustained by the fluting from out-of-plane crushing. MD transverse shear stiffness measurements were performed on the boards using the single width method as described previously to compare with the flat crush data as shown in Figure 8.

In this case, the A flute board was sent through a nip set at 70% of its original caliper, the C flute board was sent through a nip gap of 86% of its original caliper as is typically encountered by C flute boards sent through the press feed roll in the converting process. Figure 8 shows that the loss in board hardness is of the same magnitude as the loss in transverse MD shear rigidity. More data illustrating and substantiating the correspondence between flat crush hardness and out of plane shear measurements for a variety of crushed boards has been recently published (*20*). Thus measure of R_{55} is shown to be as sensitive to board crush as is the measure of flat crush hardness.

CONCLUSIONS

The measure of transverse shear has been shown to be a sensitive indicator of the quality of large-size fluted medium of corrugated board, and could be usefully exploited to evaluate the effects of flat crush in a box plant operation. Sensitivity of the measurement to board crushing is demonstrated along with corresponding flat crush hardness data. The instrument described here measures the damped oscillations of corrugated boards set into twisting motion to directly measure the MD and CD transverse shear rigidities as well as the twisting stiffness of corrugated board using a set of test samples of varying widths. The current treatment of the torsion response of the corrugated board shows that torsional stiffness such as reported in (*5*) is impacted by two mechanical properties (D_{66} and R_{55}). A measurement such as obtained in (*6*) is more indicative of only R_{55}. The results show that the full set of measurements can be utilized to distinguish the contributions of each component, for example that crushing impacts R_{55} more so than D_{66}.

For reduced testing requirements, simplified procedure using a single width of specimen and an approximation for the twisting stiffness is shown to produce similar results as the multi-width iterative method.

The analysis shows that crushing combined board will impact box strength. A significant portion of the loss in strength would not be detected by loss in ECT or bending stiffness alone. Measurement and inclusion of the transverse shear stiffness may help explain why the usual form of the McKee equation for prediction of BCT will overestimate the compression strength of boxes in many instances.

ACKNOWLEDGEMENT

The electronics and Labview™ computer programming were furnished by Theodore Jackson. Mechanical design and construction of the torsion pendulum is by Mark Urbin. The work has been funded by the IPST Consortium Members Consortium.

REFERENCES

(*1*) Urbanik T. and Frank B. – Box Compression Analysis of World-Wide Data Spanning 46 years, *Wood and Fiber Science*, **38**(3):399, 2006.
(*2*) Nordstrand T. and Carlsson L. – Evaluation of transverse shear stiffness of structural core sandwich plates *Composite Structures* **37** 145, (1997).
(*3*) McKinlay P.R. – Shear Stiffness Tester. Australian Patent 603502 (Feb 8 1989), US patent 4,958,522.
(*4*) McKinlay P.R. – Analysis of the strain field in a twisted sandwich panel with application to determining the shear stiffness of corrugated board. *Proc. 10th Fund. Res. Symp. of the Oxford and Cambridge series*, Oxford, 575 (1993).
(*5*) Chalmers I.R. – A new method for determining the shear stiffness of corrugated board, *Appita J.*, **59**(5):357 (2006).
(*6*) XQ Innovations, "BQM" Box Quality Monitor, Melbourne, Australia.
(*7*) Yoshida I., Sugai T., Tani M., Minamida K. and Hayakawa H. – Automation of Internal Friction Measurement Apparatus of Inverted Torsion Pendulum Type, *J. Phys. E: Sci. Instr.*, **14**(10):1201 (1981).
(*8*) Reissner E. – On torsion and transverse flexure of orthotropic elastic plates *J. of Appl. Mech.*, **47**, 855, (1980).
(*9*) Baum G.A., Brennan D.C. and Habeger C.C. – Orthotropic Elastic Constants of Paper, *Tappi.J.*, **64**(8):97 (1981).
(*10*) Kroeschell W.O. – The Edge Crush Test, *Tappi J.*, **75**(1) 79 (1992).
(*11*) Nordman L., Kolhonen E. and Toroi M. – Investigation of the compression of corrugated board, *Paperboard Packaging*, **63**(10):48, 1978.
(*12*) Batelka J.J. – Effect of Box Plant Operations on Corrugated-Board Edge Crush Test, *Tappi J.*, **77**(4):193, (1994).
(*13*) McKee R.C., Gander J.W. and Wachuta J.R. – Compression strength formula for corrugated boxes, *Paperboard Packaging* **48**(8):149, (1963).
(*14*) Vinson J.R. and Sierakowski R.L. – **The behavior of structures of composite materials**, Martinus Nijhoff Publishers, 1987.
(*15*) Whitney J.M. – **Structural Analysis of Laminated Anisotropic Plates**, Technomic Publishing, 1987.
(*16*) Timoshenko and Gere, **Theory of Elastic Stability**, McGraw-Hill (1961)
(*17*) Allen H.G. – **Analysis and Design of Structural Sandwich Panels,** Pergamon Press, Oxford (1969).
(*18*) Frank B. – Which ECT? C*orrugating International*, August 2003.
(*19*) Crisp C.J., Stott R.A. and Tomlinson J.C. – Resistance of Corrugated Board to flat crushing Loads *Tappi J.*, **51**(5):80A, (1968).
(*20*) Popil R. – Shear Measurement for Corrugated Board, *Paperboard Packaging*, **92**(7):37,(2007).

Appendix: Derivation of Buckling Load

Start with the constitutive relation given in Equation [2]. Take the strains to be defined as

$$\kappa_{xx} = \frac{\partial \varphi}{\partial x},\ \kappa_{yy} = \frac{\partial^2 w}{\partial y^2},\ \kappa_{xy} = \frac{\partial \varphi}{\partial y} - \frac{\partial^2 w}{\partial x \partial y},\quad \gamma_{yz} = 0,\ \text{and}\ \gamma_{xz} = \varphi + \frac{\partial w}{\partial x} \qquad \text{[A-1]}$$

where ϕ is the angle of rotation in the MD direction and w is the out-of-plane displacement. Equilibrium equations of the integrated forces are written as

$$\frac{\partial M_x}{\partial x} + \frac{\partial M_{xy}}{\partial y} - Q_x = 0 \qquad \text{[A-2]}$$

$$\frac{\partial M_{xy}}{\partial x} + \frac{\partial M_y}{\partial y} - Q_y - P\frac{\partial w}{\partial y} = 0 \qquad \text{[A-3]}$$

and

$$\frac{\partial Q_x}{\partial x} + \frac{\partial Q_y}{\partial y} = 0 \qquad \text{[A-4]}$$

Substitution of Equation [A-2] and [A-3] into [A-4] gives

$$\frac{\partial^2 M_x}{\partial x^2} + 2\frac{\partial^2 M_{xy}}{\partial x \partial y} + \frac{\partial^2 M_y}{\partial y^2} - P\frac{\partial^2 w}{\partial y^2} = 0 \qquad \text{[A-5]}$$

Substitution of Equations [2] and [A-2] into [A-5] and [A-2] gives

$$D_{11}\frac{\partial^3 \varphi}{\partial x^3} + D_{12}\left(\frac{\partial^3 \varphi}{\partial x \partial y^2} - \frac{\partial^4 w}{\partial x^2 \partial y^2}\right) + 2D_{66}\left(\frac{\partial^3 \varphi}{\partial x \partial y^2} - \frac{\partial^4 w}{\partial x^2 \partial y^2}\right) - D_{22}\frac{\partial^4 w}{\partial y^4} - P\frac{\partial^2 w}{\partial y^2} = 0 \qquad \text{[A-6]}$$

and

$$R_{55}\left(\varphi + \frac{\partial w}{\partial x}\right) - D_{11}\frac{\partial^3 \varphi}{\partial x^3} + D_{12}\frac{\partial^3 w}{\partial x \partial y^2} + D_{66}\left(\frac{\partial^2 \varphi}{\partial y^2} - \frac{\partial^3 w}{\partial x \partial y^2}\right) = 0 \qquad \text{[A-7]}$$

A solution is sought in the form

$$w = A\sin(m\pi\frac{x}{a})\sin(n\pi\frac{y}{b})$$
$$\gamma_{xz} = B\cos(m\pi\frac{x}{a})\sin(n\pi\frac{y}{b}) \qquad \text{[A-8]}$$
$$\phi = \left(B + \frac{m\pi}{a}A\right)\cos(m\pi\frac{x}{a})\sin(n\pi\frac{y}{b})$$

The Equations [A-8] are substituted into Equations [A-6] and [A-7]. Manipulation of the resulting equations gives

$$B = \frac{\pi}{a}m\frac{\left(r^2 + \alpha\right)}{R + r^2 + \beta}A \qquad \text{[A-9]}$$

and equation [13] where the symbols are defined in the main text.

Original manuscript received 3 July 2007, revision accepted 3 December 2007